PNAS
www.pnas.org

Supplementary Information for

Insights into the evolution of regulated actin dynamics via characterization of primitive gelsolin/cofilin proteins from Asgard archaea

Caner Akıl[1,2], Linh T. Tran[3], Magali Orhant-Prioux[4], Yohendran Baskaran[1], Edward Manser[1,2], Laurent Blanchoin[4,5] & Robert C. Robinson[1,3,6,*]

Email: br.okayama.u@gmail.com

This PDF file includes:

Figures S1 to S10
Tables S1
Legends for Movies S1 to S5
SI References

Other supplementary materials for this manuscript include the following:

Movies S1 to S5

www.pnas.org/cgi/doi/10.1073/pnas.2009167117

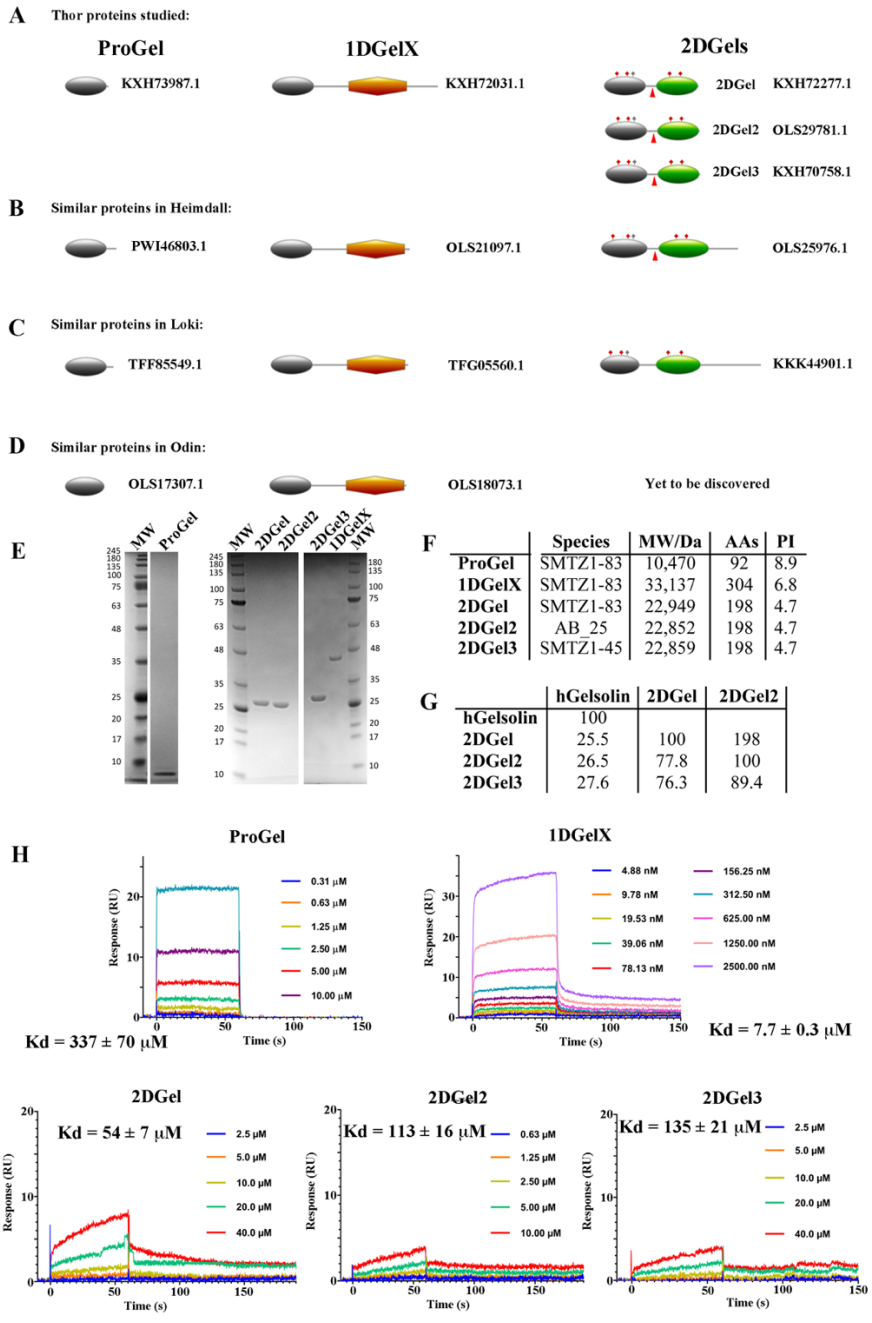

	Species	MW/Da	AAs	PI
ProGel	SMTZ1-83	10,470	92	8.9
1DGelX	SMTZ1-83	33,137	304	6.8
2DGel	SMTZ1-83	22,949	198	4.7
2DGel2	AB_25	22,852	198	4.7
2DGel3	SMTZ1-45	22,859	198	4.7

	hGelsolin	2DGel	2DGel2
hGelsolin	100		
2DGel	25.5	100	198
2DGel2	26.5	77.8	100
2DGel3	27.6	76.3	89.4

Fig. S1. Gelsolin/cofilin-like proteins in Asgard archaea. (*A*) Domain architectures and GenBank accession numbers of Thor proteins from this study. The genes encoding these proteins and actin do not form an operon in the genome assemblies. Homologous protein architectures from (*B*) Heimdall, (*C*) Loki and (*D*) Odin. Actin and profilin are also found in each of these phyla. (*E*) SDS PAGE gel demonstrating the purity of the recombinant Thor proteins. Concentrations and solution conditions are a detailed in Fig. 1. (*F*) Characteristics of the Thor proteins, including source species, molecular weight (MW), number of amino acids (AAs) and pI. (*G*) Percentage identity between the Thor 2DGels. (*H*) Surface plasmon resonance binding studies of Thor proteins to rActin. Direct binding assays were performed by covalent linkage of rActin to the sensor chip and injecting a dilution series of Thor proteins.

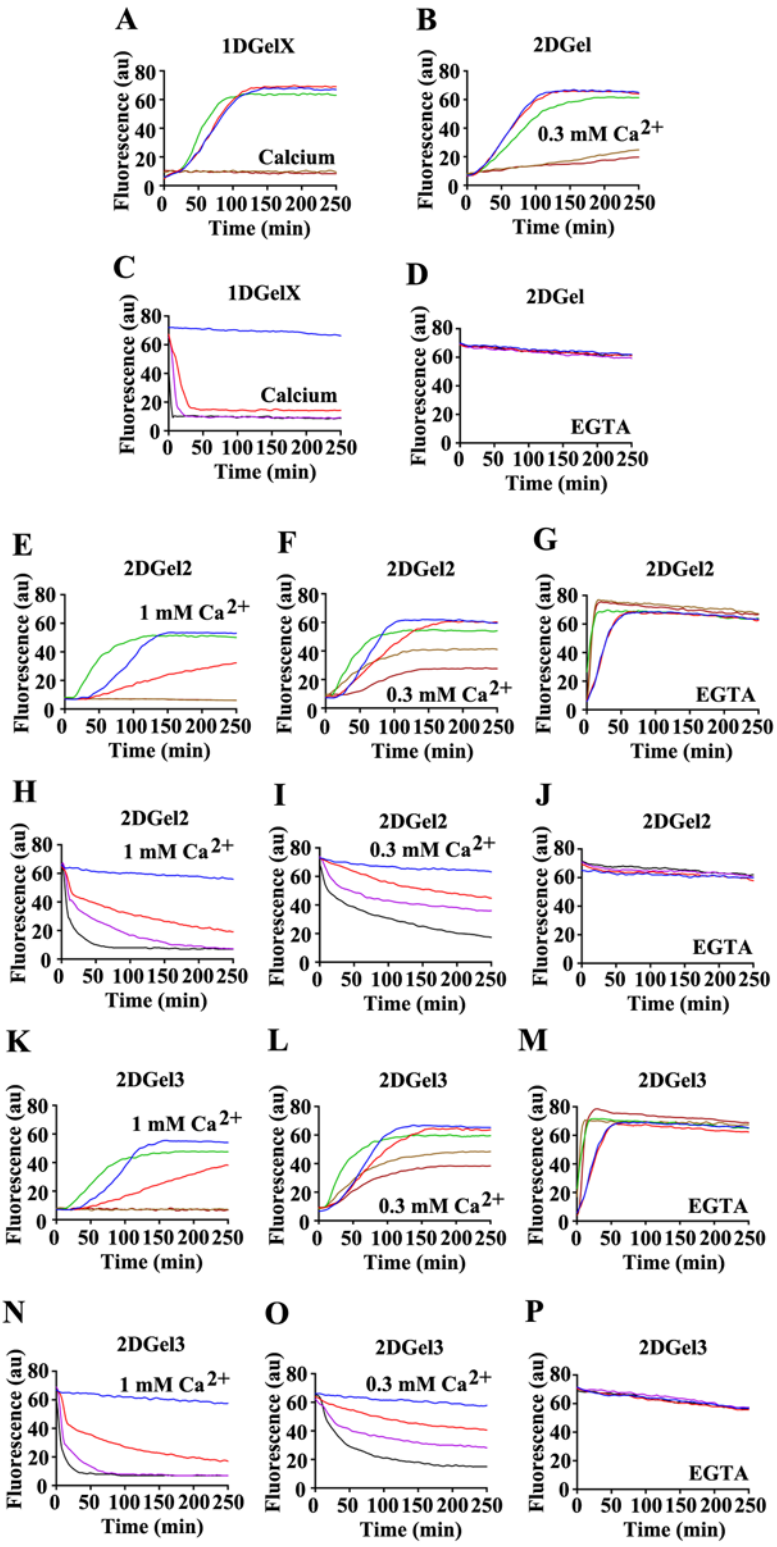

Fig. S2. Actin regulation by 2DGel2 and 2DGel3 and control experiments for Fig. 1*B-I*. Concentrations and solution conditions are a detailed in Fig. 1.

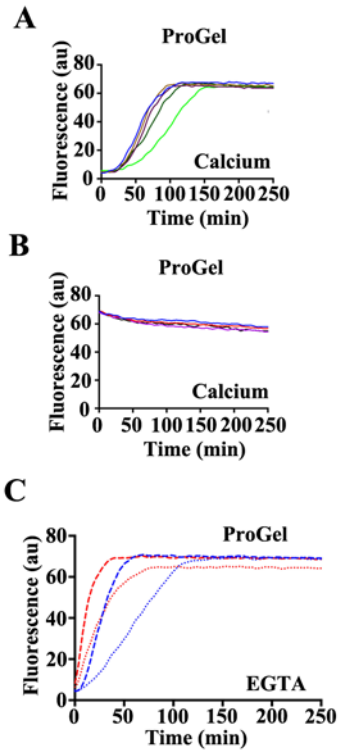

Fig. S3. Actin regulation by ProGel. (*A*,*B*) Actin regulation by ProGel in 0.3 mM Ca^{2+}, control experiments for Fig. 1*J-K*. Concentrations and solution conditions are a detailed in Fig. 1. (*C*) Pyrene-actin polymerization profiles of 2 μM actin (dashes) or 2 μM actin with 128 μM ProGel (dots) in the presence (red) or absence (blue) of actin filament seeds. The delay in fluorescence increase could be overcome by adding actin filament seeds. These data suggest that ProGel may have partial profilin-like properties, as observed for the Asgard profilins (1), in supporting filament elongation, but suppressing spontaneous actin nucleation, or may have low-level monomer sequestering or filament capping properties, and these properties are not under calcium control. However, the effects on rabbit actin are weak and Thor actin is required to confirm whether these are genuine properties of ProGel.

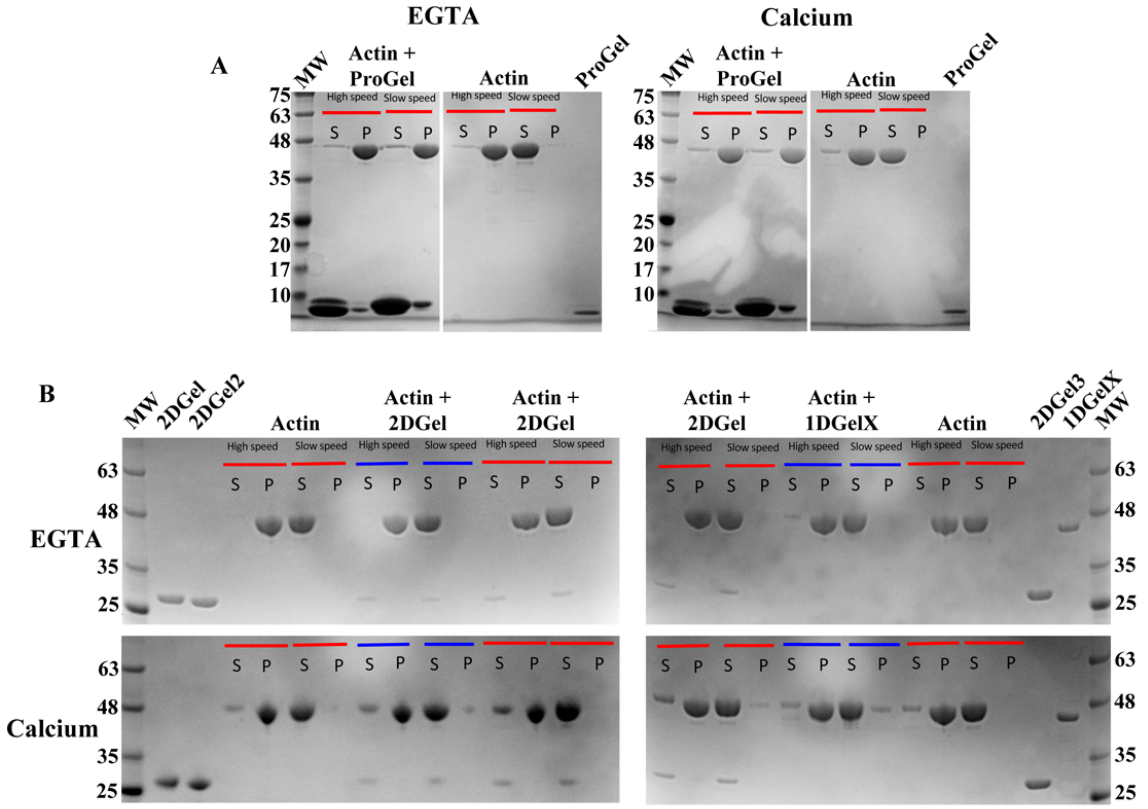

Fig. S4. F-actin in the presence of Thor proteins. (*A,B*) Sedimentation studies followed by SDS PAGE analysis of the effects of ProGel (*A*) or 2DGels (*B*) on F-actin. S = soluble fraction, P = pellet. Low speed centrifugation pellets actin filament bundles. High speed centrifugation pellets F-actin single filaments and filament bundles. ProGel pellets actin at low speed indicating bundle formation and some ProGel is observed in the pellet indicating filament binding. 2DGels and 1DGelX do not bundle filaments under these conditions and do not sediment with F-actin.

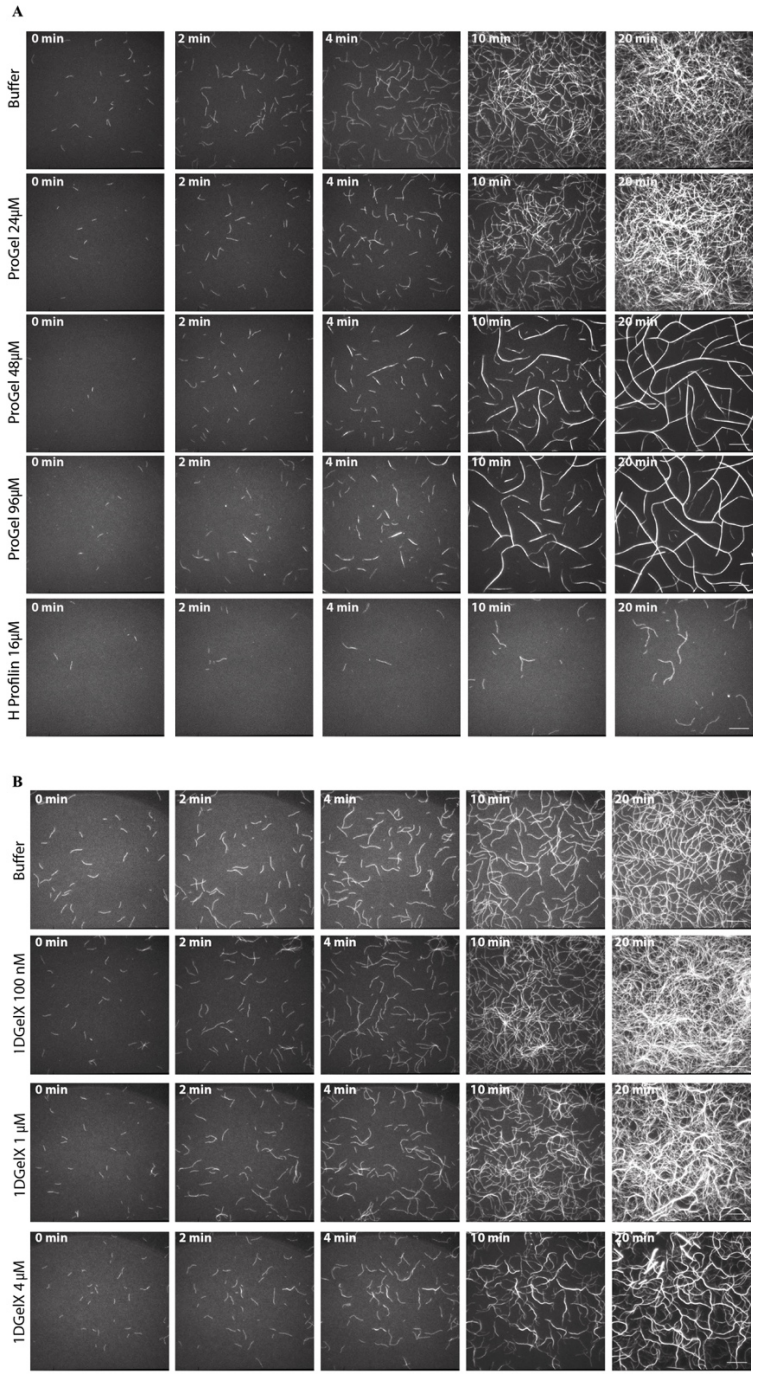

Fig. S5. Effects of ProGel and 1DGelX on actin polymerization. Time course of polymerization of 1.5 μM actin in the presence of (*A*) various concentrations of ProGel or human profilin (16 μM), (*B*) various concentrations of 1DGelX. The figures were generated from Movies S1 and S2, respectively. The scale bar represents 20 μM.

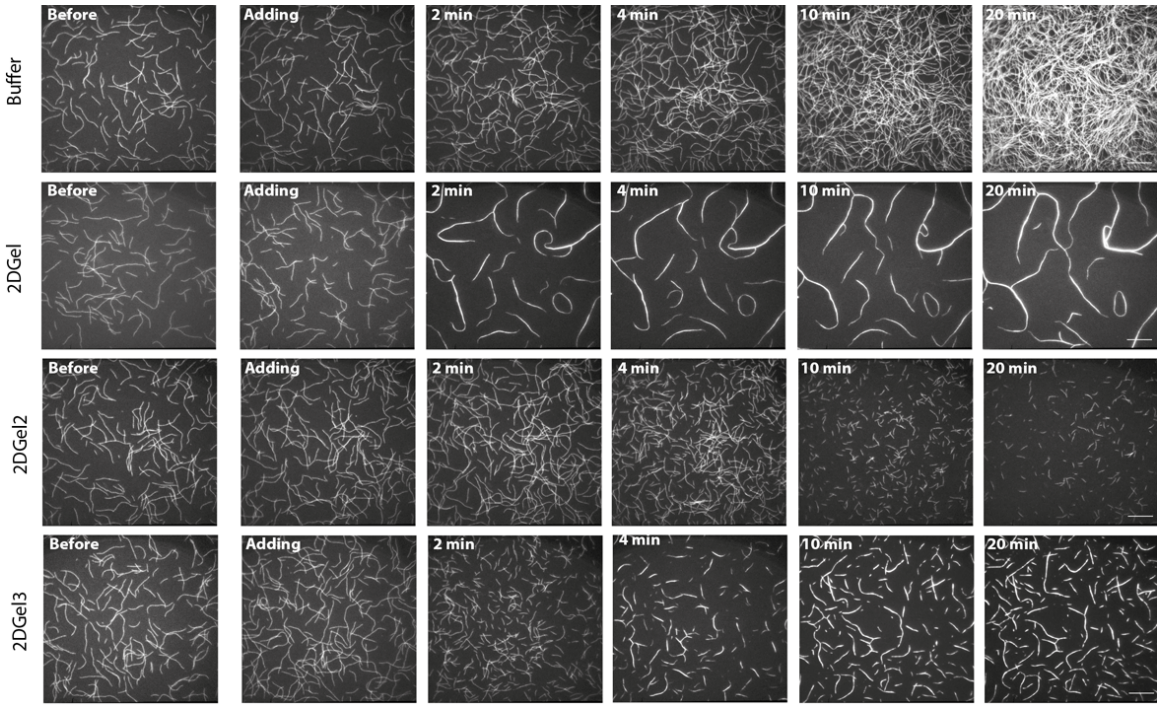

Fig. S6. Effects of 2DGel, 2DGel2 and 2DGel3 on actin depolymerization. Time course of depolymerization of 1.5 μM actin in the presence of 32 μM 2DGel proteins in 0.3 mM $CaCl_2$. The figure was generated from Movie S5. The scale bar represents 20 μM.

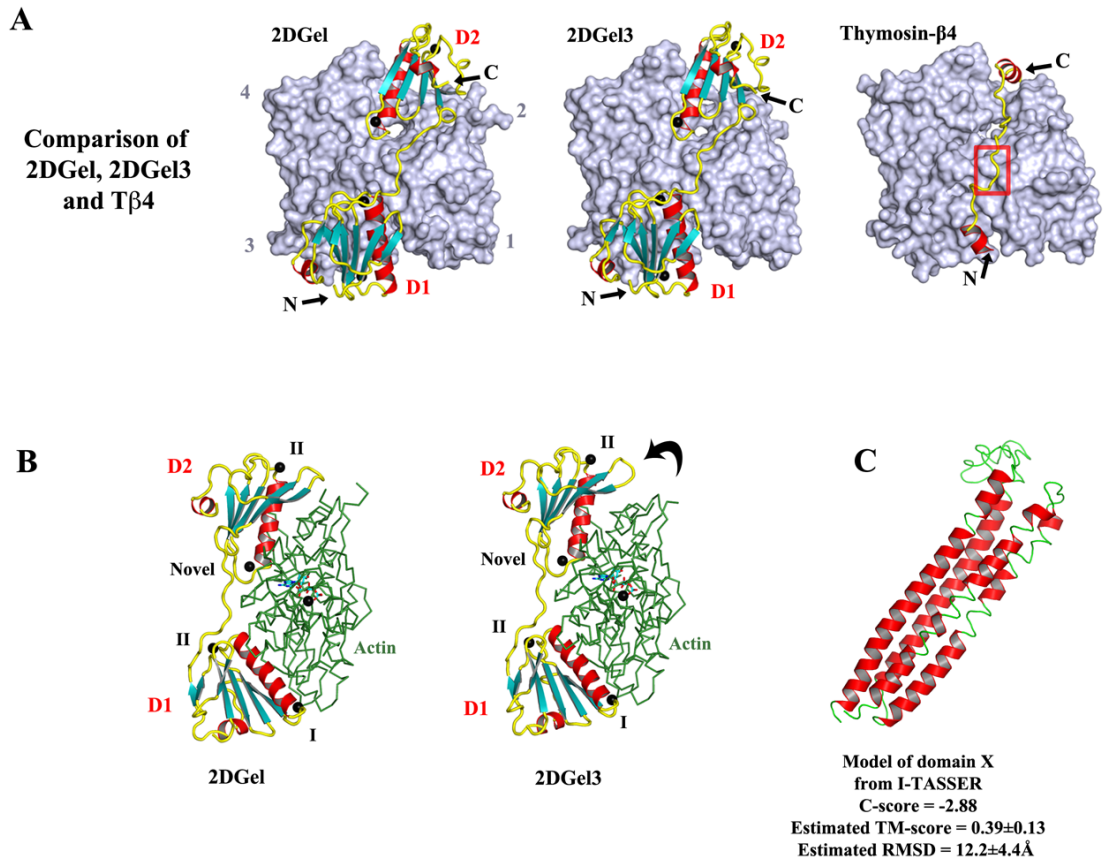

Fig. S7. Comparison of the structures of 2DGel and 2DGel3 in complex with actin. (*A*) The 2DGel, 2DGel3 (a 2DGel ortholog) and Tβ4 (PDB code 4PL7) structures in complex with actin. Actin is shown as surfaces and binding partners are shown in schematic representation. The red box indicates the position of the "LKKT" WH2-like motif on the thymosin-β4 structure. D1, D2, N, C and numbers indicate domain 1, domain 2, N-terminus, C-terminus, and the subdomains of actin, respectively. (*B*) Side on views of the 2DGel/rActin complexes. I, II and novel refer to Type I, Type II or the novel calcium-binding sites, respectively. These Type I and Type II calcium-binding sites are conserved in human gelsolin. D2 from 2DGel packs more closely to the surface of actin than D2 form 2DGel3 (indicated by the arrow), possibly providing a structural basis for the difference in activities of these proteins (Fig. S6). (*C*) Model of the structure of domain X from 1DGelX generated by I-TASSER, with statistics that suggest that the model is of low confidence (2).

A

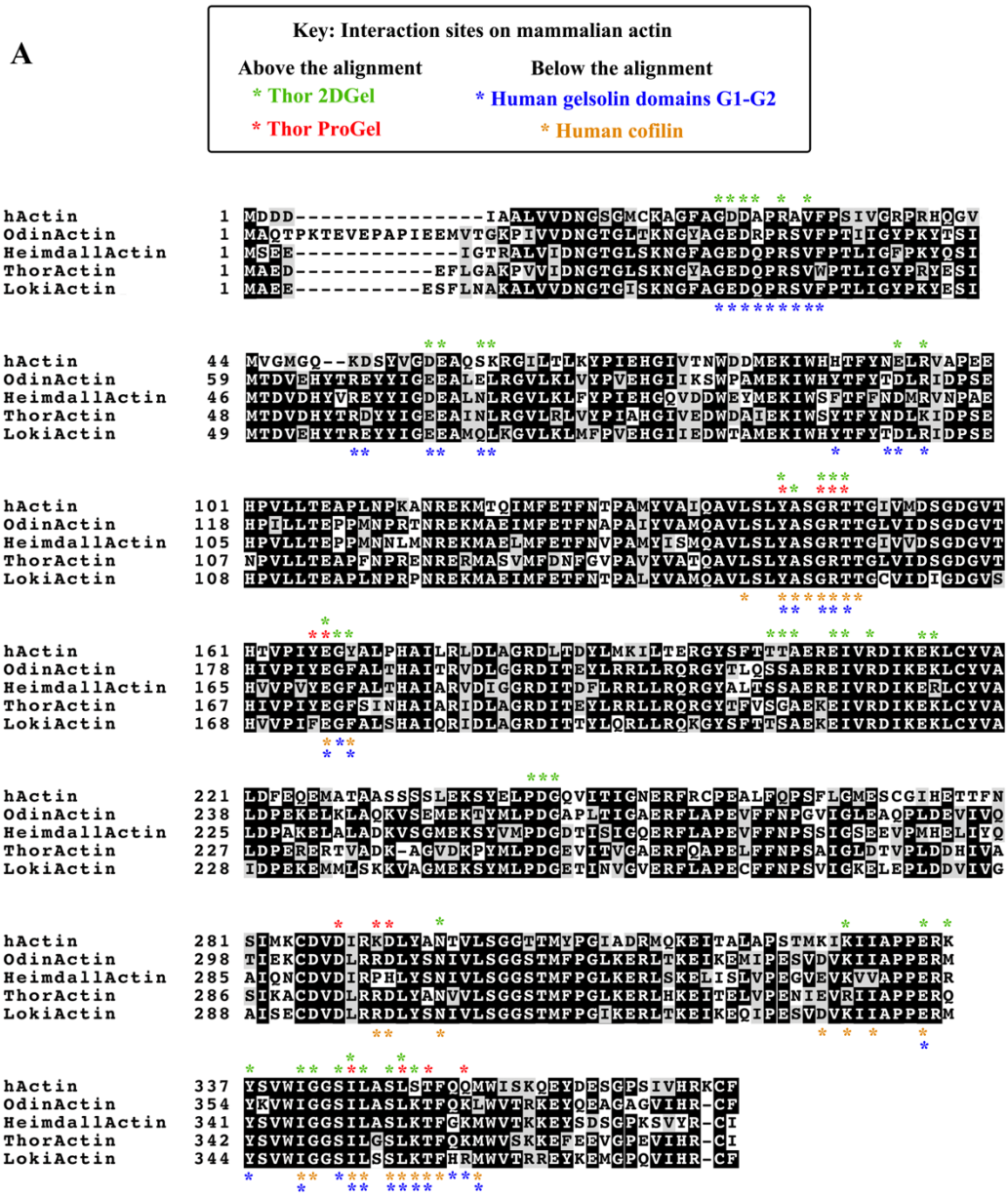
Key: Interaction sites on mammalian actin
Above the alignment
* Thor 2DGel
* Thor ProGel
Below the alignment
* Human gelsolin domains G1-G2
* Human cofilin
hActin
OdinActin
HeimdallActin
ThorActin
LokiActin

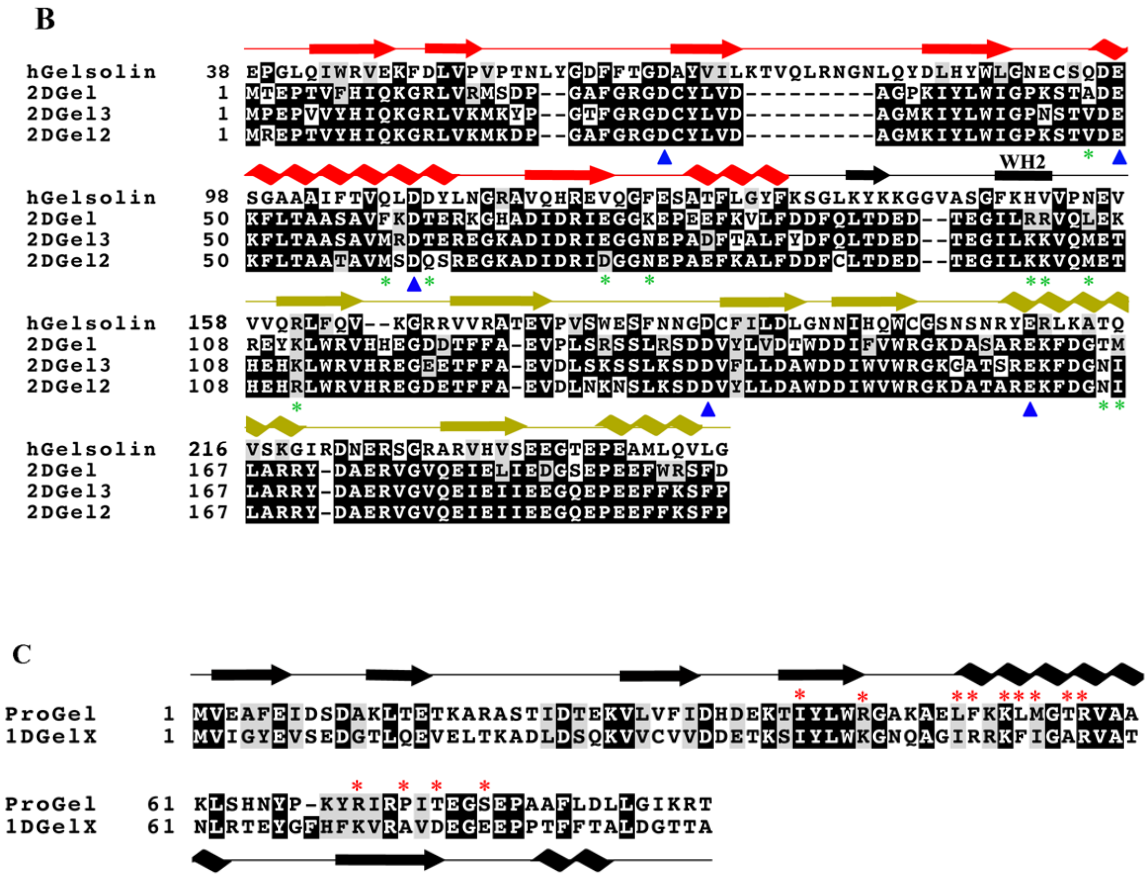

D

	hGelsolin	2DGel	2DGel2	2DGel3	ProGel	1DGelX
hGelsolin	100					
2DGel	27.6	100				
2DGel2	28.7	77.3	100			
2DGel3	28.7	80.7	85.2	100		
ProGel	12.5	20.2	21.4	21.4	100	
1DGelX	13.0	21.8	20.7	20.7	35.2	100
hCofilin	11.5	12.6	12.6	12.6	9.2	15.1

Fig. S8. Sequence alignments of (*A*) Asgard and human actin, (*B*) Thor 2DGels and human gelsolin, and (*C*) the gelsolin/cofilin domain from Thor ProGel and 1DGelX. (*A*) The binding sites of Thor ProGel and 2DGel on actin overlap with the cofilin and gelsolin binding sites (stars, refer to key) and these residues are largely conserved between Asgard actins and human actin. (*B*) Secondary structure is shown above the alignment, domain 1 (red), linker (black), domain 2 (mustard). Blue triangles = calcium-binding residues, green stars = residues in the actin-binding side that vary among 2DGel, 2DGel2 and 2DGel3. “WH2” indicates the WH2-like central motif. (*C*) Alignment of ProGel with 1DGelX. Red stars = actin-binding residues on ProGel. These are largely conserved in the 1DGelX sequence. (*D*) Percentage identities between the core D1s from the Thor proteins and human cofilin and gelsolin from structure-based sequence alignment (Fig. 4*H*).

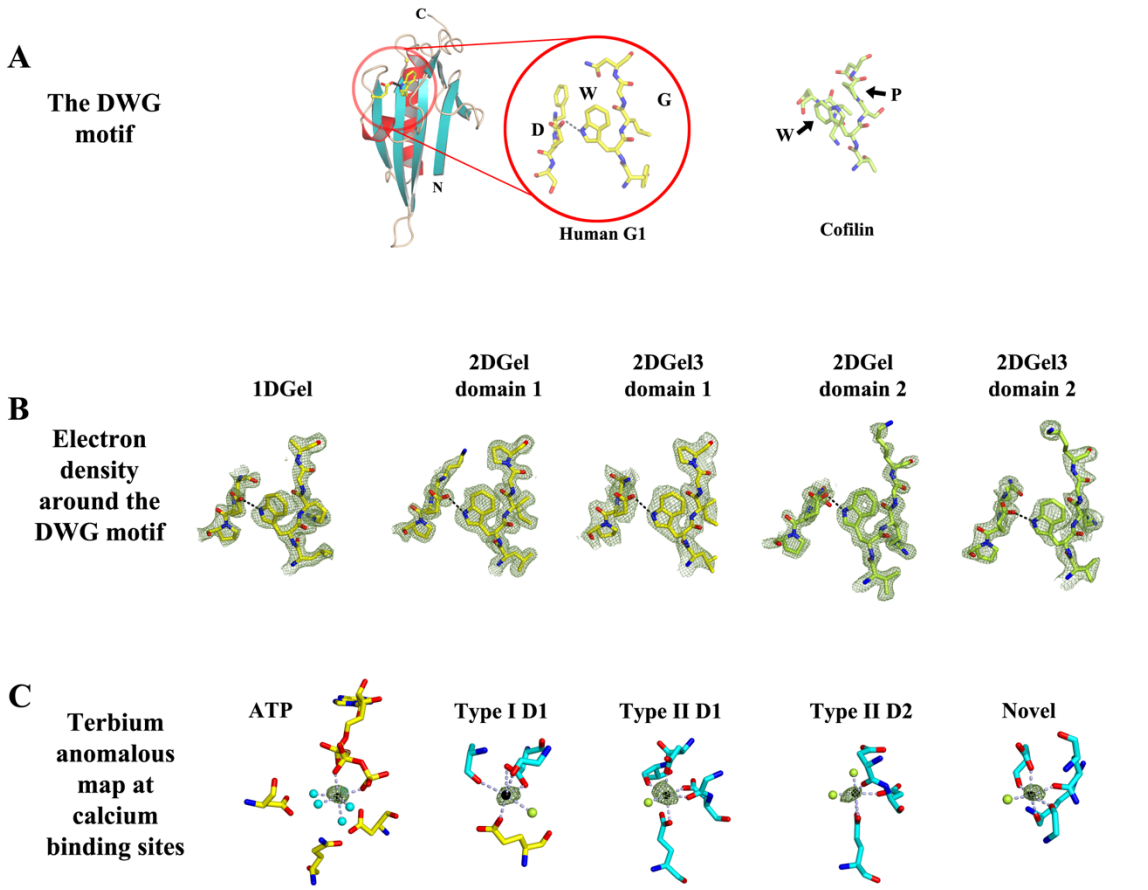

Fig. S9. The DWG motif and calcium-binding sites. (*A*) The DWG motif. The location of the DWG motif, in which the aspartic acid forms a hydrogen bond to the tryptophan which sterically occludes residues larger than glycine. This is present in all domains of human gelsolin (PDB code 3FFN) but absent from the cofilin fold, such as mouse twinfilin D2 (PDB code 3DAW). (*B*) The OMIT map electron density (contour level 1 σ) is shown around the DWG motifs from the Thor gelsolins. (*C*) The terbium anomalous difference map (contour level 6-8 σ) showing density at each of the metal ion binding sites in the 2DGel/actin complex. Actin residues are shown in yellow, 2DGel in cyan, Tb^{3+} as black spheres and waters as light green or cyan spheres.

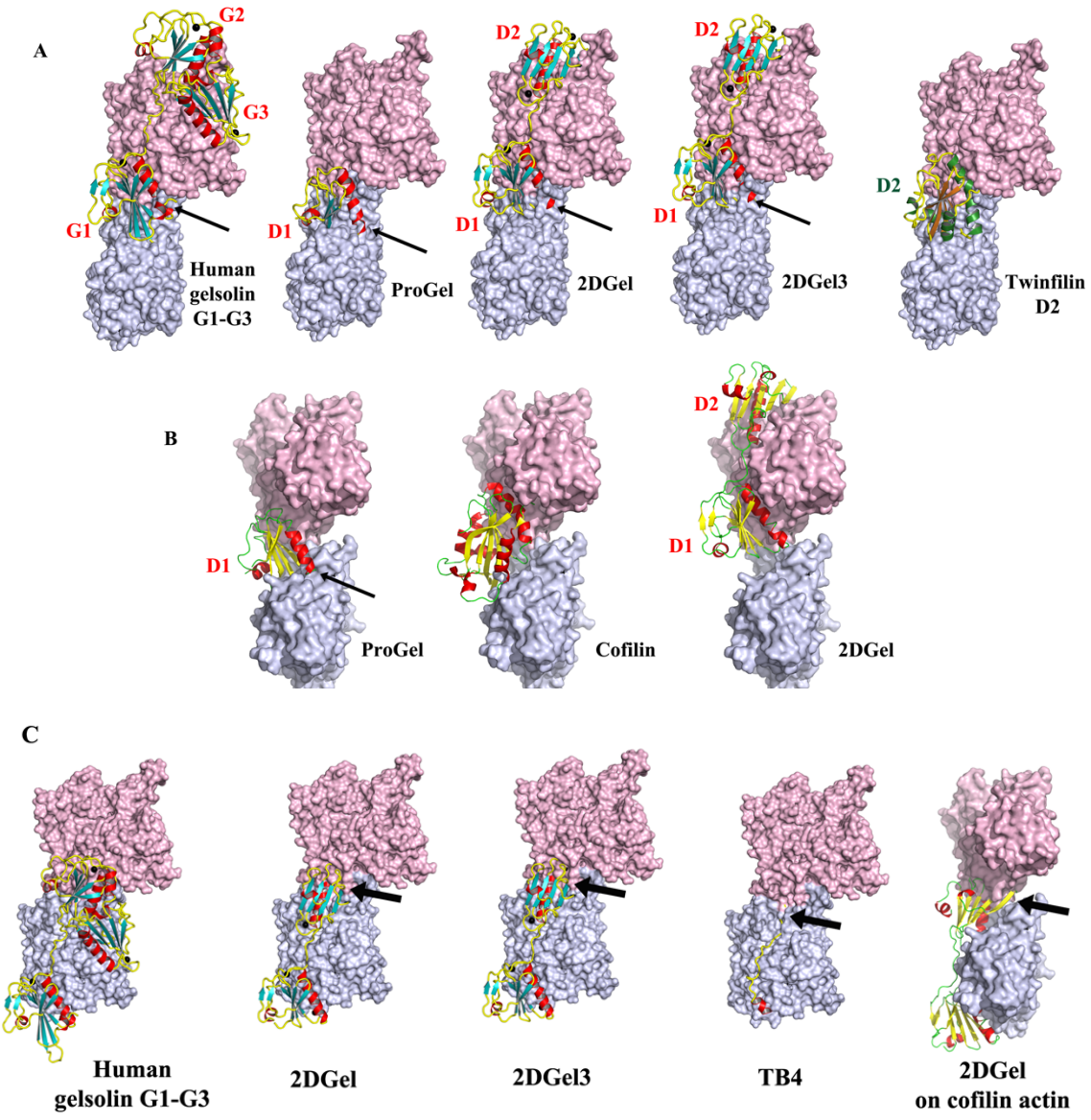

Fig. S10. Models of the Thor gelsolins bound to two subunits from F-actin. (*A*) The models were created by superimposing the actin to which each Asgard gelsolin is bound onto the cryoEM structure of the bare actin filament (PDB 3J8A) or (*B*) the cryoEM structure of the cofilin actin filament (PDB 5YU8), in each case focusing on the first domains. (*C*) Focusing on the second domains. The arrows point towards steric clashes with F-actin, indicating that these proteins are incompatible with binding F-actin in these conformations. (*A*) Predicts that G-actin bound ProGel or 2DGel/2DGel3 will be unable to join the pointed end of F-actin, while (*C*) predicts that G-actin bound 2DGel/2DGel3 will not be able to bind to the barbed end of F-actin. This is consistent with profilin-like inhibition of nucleation or barbed end capping for ProGel, and with monomer sequestration for 2DGel/2DGel3. All Thor gelsolins show at least some steric clash with the side of an actin filament, suggesting that some flexibility in the binding sites is required for severing, capping or bundling of actin filaments.

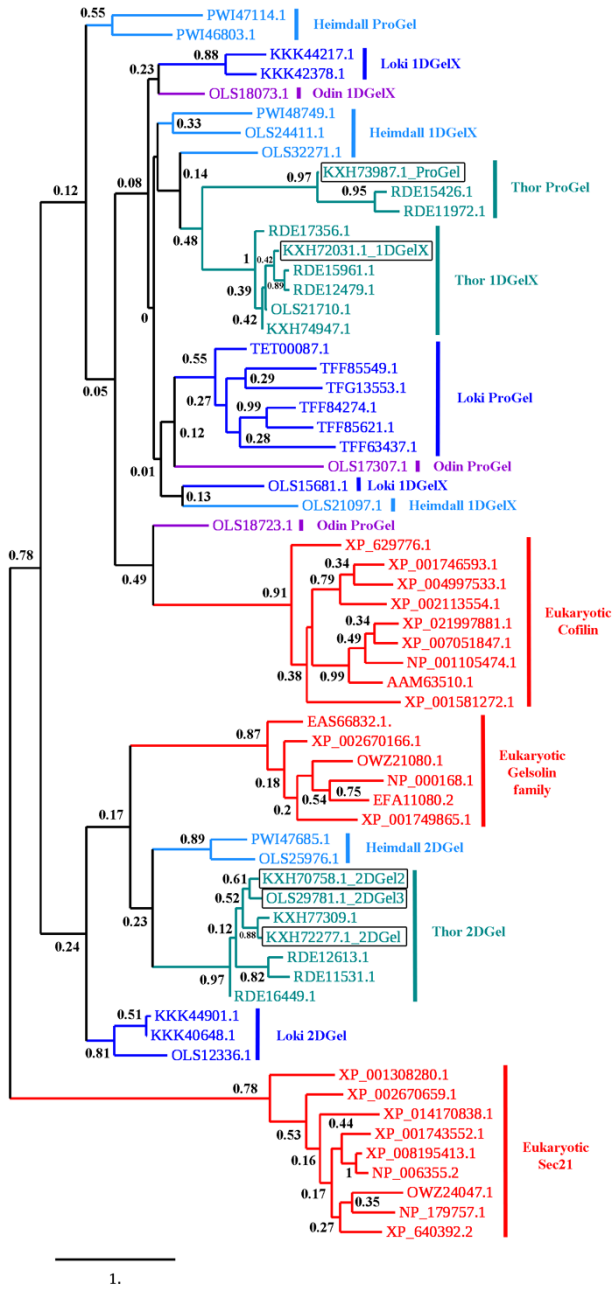

Fig. S11. Phylogenetic analysis of gelsolin/cofilin protein core sequences. The non-actin binding protein family Sec21 is an outgroup. ProGel and 1DGelX are intermingled between Asgard phyla, but are consistent within phyla, and branch close to eukaryotic cofilins. 2DGels branch with the eukaryotic gelsolin family. The support values are not statistically significant for many branches in this tree. Thus, we do not take this tree to be direct evidence for evolutionary relationships. The lack of robustness in this phylogenetic analysis may stem from several sources. These are short, diverse sequences for which, in most cases, it is unknown if distantly related sequences really represent actin or ARP interacting proteins, since their functions are untested. Distantly related sequences are subject to sequence alignment errors, which skew phylogenetic analyses. Furthermore, the actin/ARP sequences are also diverse between Asgard phyla (1). Thus, we speculate that the structure/function signature patterns are weak within these sequences leading to the lack of robustness in phylogenetic analysis.

Table S1. X-ray diffraction data collection and refinement statistics.

	ProGel/rActin (PDB code 7C2F)	2DGel/rActin (PDB code 7C2G)	2DGel3/rActin (PDB code 7C2H)
Data collection			
Crystal	$P2_12_12_1$	$P2_1$	$P2_1$
a, *b*, *c* (Å)	57.4, 108.6, 167.5	52.9, 101.3, 55.8	49.9, 98.6, 62.5
α, β, γ (°)	90.0, 90.0, 90.0	90.0, 96.6, 90.0	90.0, 94.0, 90.0
Wavelength (Å)	1.0	1.0	1.0
Resolution (Å)[a]	91.1-2.03 (2.08-2.03)	20.0-1.71 (1.73-1.70)	31.2-2.35 (2.44-2.35)
R_{merge}	11.5 (79.0)	10.0 (92.3)	13.5 (58.4)
R_{meas}	12,5 (85.6)	10.8 (108.0)	14.4 (64.3)
R_{pim}	4.8 (32.7)	4.2 (45.5)	5.5 (26.3)
$I/\sigma(I)$	8.6 (1.8)	20.1 (1.8)	17.3 (2.3)
$CC_{1/2}$	0.998 (0.785)	0.926 (0.632)	0.946 (0.862)
Completeness (%)	99.5 (93.0)	98.0 (92.5)	92.4 (81.4)
Redundancy	6.7 (6.6)	6.6 (4.5)	6.8 (5.5)
Refinement			
Resolution (Å)	48.6-2.03 (2.10-2.03)	20-1.71 (1.74-1.70)	31.2-2.35 (2.48-2.35)
No. reflections	68184 (6521)	58175 (1354)	23279 (2562)
R_{work} / R_{free}	20.0/23.0 (27.1/29.45)	16.9/20.3 (22.4/26.4)	20.2/23.8 (29.6/34.2)
No. atoms*			
Protein	5704 (A)/1428 (G)	2943 (A)/1620 (G)	2823 (A)/1615 (G)
Ligand/ion	116 (LatB, ATP)/2 (Mg^{2+})	31 (ATP)/7 (Ca^{2+})	31 (ATP)/6 (Ca^{2+})
Water	567	557	124
B factors			
Protein	42.3/82.1#	33.5/37.0	45.2/52.4
Ligand/ion	26.0/21.7	26.0/18.9	36.2/45.2
Water	43.1	36.9	48.6
r.m.s deviations			
Bond lengths (Å)	0.003	0.007	0.009
Bond angles (°)	0.75	0.88	1.05
Ramachandran Plot			
Favoured (%)	97.7	97	98
Outliers (%)	0.11	0	0

* ProGel/rActin has 2 complexes in the asymmetric unit.
# The B-factors of ProGel are approximately 2 times that of rActin in this complex. This is likely the product of fewer crystal contacts and the poor affinity of ProGel for rActin, resulting in clearer electron density for rActin relative to ProGel.

Movie S1 (separate file). Time course of polymerization of 1.5 μM actin supplemented by buffer, ProGel (24 μM), ProGel (48 μM) or ProGel (96 μM). ProGel (24 μM) shows slightly reduced polymerization relative to the control. ProGel at 48 μM and 96 μM shows bundling and annealing. All movies are sped up 200 times.

Movie S2 (separate file). Time course of the polymerization of 1.5 μM actin in the presence of buffer, 1DGelX (100 nM), 1DGelX (1 μM), or 1DGelX (4 μM). 1DGelX at 100 nM shows filament nucleation. 1DGelX at 1 μM and 4 μM show increasing levels of bundling.

Movie S3 (separate file). Time course of the polymerization of 1.5 μM actin in the presence of buffer, 2DGel (32 μM) and 1 mM EGTA, or 2DGel (32 μM) and 1 mM $CaCl_2$. 2DGel in the 1 mM $CaCl_2$ shows reduced polymerization and bundling in comparison to the presence of 1 mM EGTA.

Movie S4 (separate file). Disassembly of polymerized actin (1.5 μM) produced by 1DGelX (4 μM) in comparison to the buffer control. 1DGelX shows single filament severing, bundling followed by bundle severing.

Movie S5 (separate file). Polymerized actin (1.5 μM) in the presence of 0.3 mM $CaCl_2$ supplemented by buffer, 2DGel (32 μM), 2DGel2 (32 μM) or 2DGel3 (32 μM). 2DGel shows bundling, 2DGel2 shows single filament severing, and 2DGel3 shows single filament severing followed by bundling.

SI References

1. Akil C & Robinson RC (2018) Genomes of Asgard archaea encode profilins that regulate actin. *Nature* 562(7727):439-443.
2. Yang J & Zhang Y (2015) I-TASSER server: new development for protein structure and function predictions. *Nucleic Acids Res* 43(W1):W174-181.